^{1}H and ^{13}C NMR , FTIR spectral, and elemental analysis. The synthesis route of the ligand is shown in scheme (1).The microanalysis of results for the ligand [TmAB] and the complexes some of its physical properties are given in Table (1).

General synthesis of mixed ligands complexes

An ethanolic solution (25ml) of metal salts of Co((II), Mn(II), Fe(II), Cu(II), Ni(II), and Zn(II)was added gradually to a stirred ethanolic solution of Schiff base(25ml) and secondary ligand 1,10-phenthroline in ethanol. Few drops of KOH solution were added to adjust the pH>9. The resulting solution was refluxed for about 2 hours. The chelate was precipitated, cooled and then filtered. The result got by washed with small amounts of ethanol and dried. The microanalysis of results for the ligand and some of its physical properties are given in Table (1)

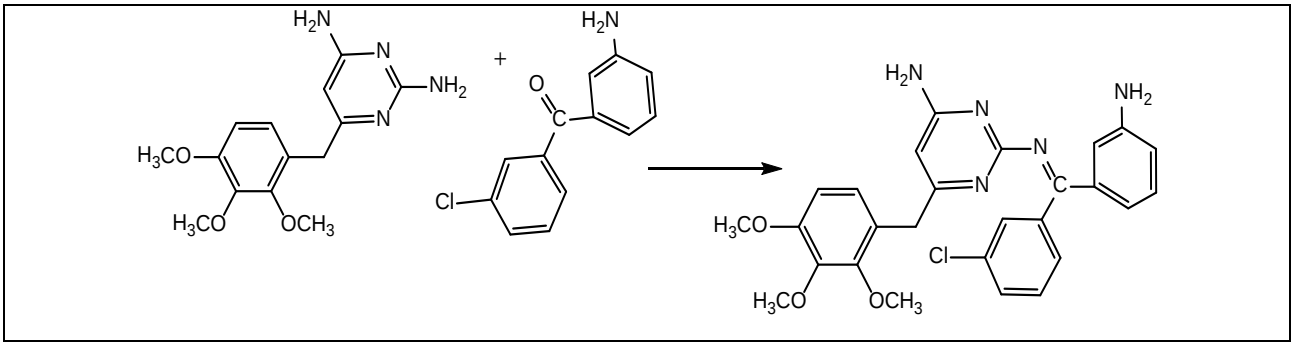

Scheme (1): preparation course of The Schiff base

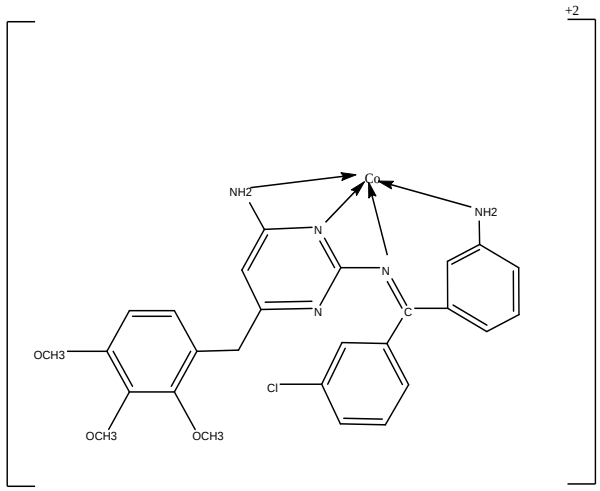

M= Mn(II), Co(II)and Cu (II)

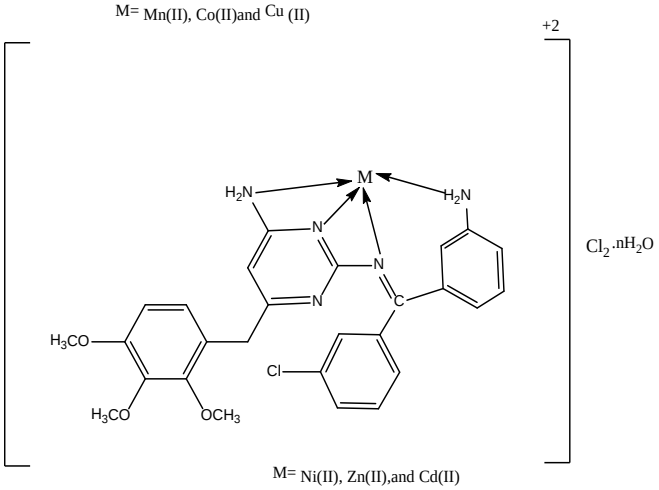

M= Ni(II), Zn(II),and Cd(II)

Antimicrobial assay

Stock cultures were maintained at 4 °C on Nutrient agar Slant. Active cultures for experiments were prepared by transferring a loop full of culture from the stock cultures into the test tubes containing nutrient broth, that were incubated for 24 hrs at 37 ºC. The assay was performed by the agar disc diffusion method. Antibacterial activity of extracts was determined by disc diffusion method on Muller Hinton agar (MHA) medium. Muller Hinton Agar (MHA) medium is poured into the Petri plate. After the medium was solidified, the inoculums were spread on the solid plates with a sterile swab moistened with the bacterial suspension (Staphylococcus aureus, Salmonella spp., E. coli, Vibrio spp., Pseudomonas aeroginosa, Vibrio parahaemolytics, Aeromonas spp., Klebsiella spp., Proteus spp., and Bacillus spp.). The disc was put in 20 µl of the samples and MHA plates (Concentration: 500 µg, 750 µg and 1000 µg) were put in the disc.

Antifungal activity assay

The Assay was performed by the agar disc diffusion method. The Antifungal efficiency of the extracts was determined by disc diffusion method on (SDA) Sabouraud Dextrose agar medium. Sabouraud Dextrose agar (SDA) medium is poured into the Petri plate. After the medium had been solidified, the inoculums were spread on the solid plates with a sterile swab moistened with the fungal suspension (Aspergillus flavus, Aspergillus niger, Pencillium spp., Candida albicans, Trichophyton). The disc was placed in SDA plates and added 20 µl of the sample (Concentration: 500µg, 750µg and 1000µg) were put in the disc. The plates were incubated for 24 hrs at room temperature. Then the antifungal activity was measured by determining the diameter of the zone of inhibition inhibits the bacterial and fungal growth compared with the control was recorded as MIC

In vitro antimicrobial activity

The methods of agar well-diffusion were used to evaluate the recently synthesized compounds. All the cultures of microbial were detected to standard (0.5 McFarland), that is visually analogous to suspension of the microbial almost 1.5 × 108 cfu/ml.

Medium of Muller Hinton agar about 20 ml were casted into each Petri plate and plates were wiped with 50 µ L inoculate of the screen bacteria and preserved for adsorption utilizing sterile cork borer of 10 mm diameter for 10min.and the wells were bored into the seeded agar plates and these were loaded with a 50µl of each compound in 4.0 mg/ml reconstructed in DMSO. All the plates were incubated °C for 24 hrs at 37. Ambit reader was applied to measure the diameter of (antibiotic ambit scale) inhibition ambit of the exam creatures. Ciprofloxacin was applied as a positive hegemony, while DMSO was applied as negative hegemony. This execution was reiterated thrice for each microbial

2.3.3. Minimum inhibitory concentration (MIC)

Promising antimicrobial leverages are offer for compounds which chosen to experience their MIC data. MIC of the deferent compounds versus microbial stains was screened through a modulated agar well-diffusion technique.

In vitro cytotoxicity

The MTT testing has been selected to esteem the in vitro cytotoxic influence of the newly synthesized Schiff base [TMAB] and its Co (II), Mn(II), Ni(II), Cu(II), Cd(II), Zn(II) complexes. This is a rapid, inexpensive, efficient screen and has a good linkage with cytotoxic activity**.**

In vitro assay for anticancer activity (MTT assay)

Cells (1×10^5/well) were painted in well plates about 24 and brooded 5 with % CO_2 in 37 °C states. When the cell arrives the junction, the samples with the different concentrations were append and brooded for 24 hrs. After brood, the model washed after removing it from the wall using MEM without serum or phosphate-buffered saline (pH 7.4).And by addendum (MTT) about (5 mg/ml) 100 µl/well (0.5%) and incubation for 4 hrs. after incubation 1 ml of DMSO, compiled in all the wells. By employing a UV-Spectrophotometer apparatus which was calculated the absorbance with the blank of DMSO at 570 nm. Gauges were performed and the coveted concentration was standardized graphically for (IC50) a 50% inhibition. The (% cell viability) was calculated employing the following formula:

% cell viability = A570 of treated cells/A570 of control cells × 100

Graphs are designed employing between Y-axis is the percentage of Cell Viability and X-axis is the sample concentration. Cell control and sample control is included in each checking to compare anti-cancer efficacy appreciations and the overall cell viability in cytotoxicity

RESULTS AND DISCUSSION:

Trimethoprim was treated with 5-chloro-2-aminobenzophenone to result a new ligand (Z)-2-(((3-aminophenyl)(3-chlorophenyl)methylene)amino)-6-(2,3,4-trimethoxy benzyl)pyrimidin-4-amine. Schiff base was subjected to reactions with $CoCl_2.6H_2O$ /$MnCl_2.4H_2O$/ $ZnCl_2$/$CdCl_2$/$CuCl_2.2H_2O$and $NiCl_2.6H_2O$ metals in ethanol to produce a series of four geometry in solution to air even. The compositions of complexes have been confirmed by microanalytical values [4].

Mass Spectra:

Mass spectrometry is a substantial gadget generally utilized for the description of chelation components [5]. Mass spectra of all the components understand in good harmonization with the suggested framework. A molecular ion peak $[M^+]$ at m/z = 503 is noticed, equivalent to its molecular weight that coincides to its molecular formula, $C_{27}H_{26}ClN_5O_3$. The fragmentation peaks observed at m/z 487, 472, 442, 413, 382, 292, 182, 106 and 77 are observed to the cleavage of $[C_{27}H_{24}ClN_4O_3]^+$, $[C_{27}H_{23}ClN_3O_3]^+$, $[C_{26}H_{22}ClN_3O_2]^+$,$[C_{25}H_{19}ClN_3O]^+$, $[C_{24}H_{17}ClN_3]^+$, $[C_{17}H_{11}ClN_3]^+$, $[C_{11}H_8N_3]^+$, $[C_5H_4N_3]$ and $[C_6H_5]^+$ respectively [6].

Nuclear magnetic resonance spectra

Supplemental constructional acquaintance can be suggested from the ^1H and ^{13}C NMR spectra. The ^1H-NMR spectra of

free ligand (TMAB) is registered in DMSO-d_6 solution using the internal standard as (TMS) [7]. ^{1}H-NMR spectrum of ligand displays multiplet at 7.01–8.46ppm resulted to the existence of aromatic protons. There is a singlet at 3.81 ppm feature of CH_2 proton. The ^{1}H NMR peaks of NH_2 protons of amine is normally expected to be present at 5.18 and 5.98 ppm. However, in the ^{1}H NMR spectrum of ligand, a supplemental singlet observes between 3.70 and 3.77ppm and 3.83ppm pertaining to the CH_3 of the ligand respectively.

The ^{13}C NMR spectrum of ligand offers aromatic carbon peaks in the range 118.5-142.8 ppm. It also displays another important signal at 167.3 ppm, advantage of C=N bond [8].

Thermal analyses studies of metal complexes:

Thermal behavior and thermal stability of all the metal chelate were presented by (TGA) thermo- gravimetric analyses in in range 30-850 of the temperature °C. The thermogram of the IF_1 displays a mass removal of 3.01 % (calcd. 2.47 %) of the temperature range 82-113°C evidences the lack of one molecule of Lattice water. The second stage of the deterioration from 130-230 °C, with a mass lack of 9.51 % (calcd. 9.77 %) coincides to lack of the coordinated two amine and three methanol molecules, the 3rd stage includes in the dissociation at the temperature of 260-400°C with weight lack of 35.66 %(calcd. 28.99 %) corresponds to the deterioration of benzene moiety [9]. The 4th stage at 410-690 °C with weight loss of found 42.79 % (calcd. 49.07 %) is suggesting to the loss of pyridine moiety and at the end, left behind stable residue NiO (9.09 % (calcd. 10.28 %) at 690-740 °C. Correspondingly, the TG curve of the IF_2 to IF_5 displays three-steps of decomposition. The first stage with weight lack of 13.54, 13.11, 16.13 , 14.23 and 11.35% (calcd. 12.92, 12.56, 12.85, 13.11 and 13.08 %) at 170-240, 140-220, 180-270 and 160-260°C, respectively is coincided to the lack of molecule of water and two chlorine atoms, the 2nd stage with weight lack of 38.12 , 38.79, 39.06, 39.23 and 39.98 % (calcd. 37.29, 37.43, 38.14, 38.34 and 38.56 %) at 250-390, 230-290, 280-390 and 260-370 °C was coinciding to the removal of aniline moiety and trimethoxy benzene moiety from the chelated ligand [9]. The 3rd stage at 310-680, 320-700, 410-700 and 320-400 °C with weight lack of 39.56, 39.76, 39.98, 40.02 40.34 and 40.56 %, respectively (calcd. 38.23, 38.39, 38.48, 39.02, 39.34 and 39.78%) is referring to the removal of pyridine moiety chlorobenzene moiety .The mass of the final residue 14.45, 14.76, 15.22, 15.47 and 15.94 % (calcd.13.26 ,13.80, 14.33 , 14.78 and 14.96 %) at 690-720, 790-740,710-740 and 600-750°C coincided to constant MnO, CoO, NiO, CuO, ZnO , and CdO respectively [10]. The outcomes well concordant with the dismantling of the metal complexes.

IR spectra

IR spectra of the complexes obviously signalize the bonding combination of the metal ion with the ligand. Generally the IR spectra of the Schiff base show a two bands around 3421 and 3377 cm^{-1} which can be attributed of the incorporation υ_{sym} and $_{asy}$ (NH_2) stretching vibrations [11] .The position of this band shifts to higher frequency in the spectra of the metal complexes indicating the coordination of these nitrogen's of amine groups. In the IR spectrum of a Schiff base ligand or complex, the ultimate considerable signal is the stretching frequency of the(C=N) imine moiety. This signal usually transfers to lower wavenumbers upon chelation of nitrogen of the imine to the ion of the transition metal [12]. In the ligand spectrum, the existence, of an intense band at ~ 1597 cm^{-1} was already attributed to the stretching frequency of the(C=N) imine moiety. In the complexes spectral, these signals transferred to lower frequencies suggesting signalizing the conjunction of the nitrogen atoms of the C=N moieties in chelation. Occurrence of a broad signal in 3081 to 3363 cm^{-1} range was noticed in the spectra of metal complexes signalizing the existence of chelated or lattice water molecules. The frequencies in the reign 788–836 cm^{-1} evidenced in the complexes spectra that may be designated to $\partial(H_2O)$ [13].

The spectrum of free ligand observed a frequency in the range 1638cm^{-1} advantages of the (azmothine) $\upsilon_{C=N}$ stretching vibration signalizing the consistency of the Schiff base output. This single was moved toward lower wavenumbers in the spectrum of its metal complexes (1620–1627)cm^{-1} contrasted with the above ligand signalizing the involvement of the azomethine nitrogen in coordination with metal ion [14]. The coordination of nitrogen to the metal ion could be expected to reduce the electron density of the azomethine link and thus caused a shift in the υ C=N moiety. A strong frequency was observed in range (1702-1708) cm^{-1} harmonizes to C-Cl bond. Incisive guide of the linking was likewise allowed by the monitoring that new signals in the spectra of all metal complexes showing in the low wavenumber ranges at 580–489cm^{-1} and 470–427cm^{-1} characteristic to υ (M–O) and υ(M–N) stretching modes, respectively [15].

Electronic spectra, Magnetic moments and conductivity measurements:

The electronic spectrum of ligand [TMAB] offered high intense absorption signal at 35842 cm^{-1} with a shoulder at 28985cm^{-1} which due to ($\pi\rightarrow\pi^*$) and ($n\rightarrow\pi^*$) transitions, respectively [16]. These bands are shifted to 36101-37453cm^{-1}, respectively, which can be attributed to the binding of these coordination centers to the central metal ions. The UV–vis spectra of the complexes display bands at 316, 500 and 670 nm which can be attributed to d–d transition within Zn(II), Mn(II), Cu(II), Ni(II), Cd(II) and Co(II) complexes, respectively. The values registered in Table (5). The electronic spectrum of the Co(II) complex displayed four signals at 29940, 24937,14556 and 13123 cm^{-1}, the first signal attributed to charge transfer and the last three signals transferable corresponding to $^4T_{1g(F)} \rightarrow {}^4A_{2g(P)}$ (υ_3), $^4T_{1g(F)} \rightarrow {}^4A_{2g(F)}$ (υ_2) and $^4T_{1g(F)} \rightarrow {}^4T_{2g(F)}$ (υ_1), transferences of octahedral structure and also more confirmed by its υ_2/υ_1 that founds in the range 1.80–2.20 [17]. The parameters of ligand field have been determined by employed the neutralization. The B data was determined and gave to be 718 cm^{-1}. The B data is lower than the Co^{2+} free ion data B$'$ (968cm^{-1}) that founds notification about d-orbital delocalization and the overlapping of orbitals. The nephelauxetic influence supposes that the lower the data of

β the higher is the range of covalence [18]. β data for Co(II) complex is less than one that supplies the notification of ligand-metal bond is covalent nature. The Ni(II) complex evidence peaks around 28985, 24509 and 12345 cm^{-1} corresponding to charge transfer, $^3A_{2g(F)} \rightarrow ^3T_{1g(P)}$ (υ_3) and $^3A_{2g(F)} \rightarrow ^3T_{1g(F)}$ (υ_2) transferences distinctive of octahedral structure. Furthermore it is more confirmed by υ_2/υ_1 being amounting to 1.68. This data is less than the υ_2/υ_1 data of 1.80 attributed for the regular octahedral Ni(II)complex . The less of data in the existing state may be observed to the asymmetric medium around Ni(II) of the complex [19]. The B data for the complex is 845 cm^{-1}. This data is lesser than the free ion value B′ (1021 cm^{-1} for Ni^{2+}) which gives information about the overlapping of orbitals and d-orbital delocalization. The covalent factor β equal to B=B′ (B = complex value and B′ = free ion data) for the complex is lower than one. While, the Cu(II) complex four signals at 29673, 24271, 14265 and 11641cm^{-1} the first signal attributed to charge transfer and the last three signals observed to $^2B_{1g} \rightarrow ^2A_{1g}$, $^2B_{1g} \rightarrow ^2B_{2g}$ and $^2B_{1g} \rightarrow ^2E_g$ transferences , respectively distinctive of distorted octahedral structure and these signals were overlap to found the three peaks in the spectrum of Cu(II) complex [20].

The electronic spectrum of Mn (II) complex showed two intense peaks in 37037 and **29940** cm^{-1}were assigned to the ligand field and transfer transition respectively. .And the peak at visible region at 24937, 14556 and 13123 cm^{-1}. These peaks are assigned to ($^4T_1g_{(F)} \rightarrow ^4A_2g_{(P)}$, $^4T_1g_{(F)} \rightarrow ^4A_2g_{(F)}$ and $^4T_1g_{(F)} \rightarrow ^4T_2g_{(F)}$) (d-d) transitions confirming an octahedral structure around (Mn^{+2}) ion complex[21]. The electronic spectra of the Zn(II) and Cd(II) complexes does not appear any d → d transition, which may be due to d^{10} electronic configuration. It has been reported that tetrahedral is the most favored one. The electronic transition spectrum of the yellow Zn(II) complex shows shoulder band at 316 nm. This band can be attributed to the LMCT transition and it is consistent with octahedral geometry [22]. The magnetic moment outcomes of transition metal complexes allow an indication of the environment of the ligand around the central metal ion. The and Cd(II) complexes are found to be diamagnetic as expected for d^{10} configuration, The Co(II), Mn(II), Ni(II), and Cu(II) complex is paramagnetic. The magnetic measurements for Co(II), Mn(II) and Cu(II) complexes showed magnetic susceptibility data of 4.72, 5.67 and 1.83 B.M., respectively, indicating uniformity with their octahedral [23].

Effect of ligand and metal complexes on antimicrobial study

The values of the antifungal and antibacterial efficacies of the compounds are sited in table 1 and 2. The antimicrobial an efficacy was calculated by standardizing the diameter of the region of suppression (fig. 1). The value detects that the complexes have higher inhibitory efficacies than the free Schiff base. The boost of the efficacy of ligand on complexation can be elucidated by Chelation Theory and Overtone's Concept. This theory declares that coordination decreases the polarity of the metal atom by the fractional involvement of its positive charge with possible π-electron delocalization over the full ring and donor moieties. This outcomes in rising lipophilic advantage of the complex and support the breakthrough of the complex through the lipid stratum of the cell membrane. The complex blocks the metal binding sites in the enzymes of bacteria. Thus, the complex disturbs the metabolism routes in the cell, producing in the extinction of microorganisms [24]. The method of activity of the compounds may include the fashioning of a hydrogen bond through the azomethine moiety (C=N–) with the energetic centers of different cellular constituents, processing in involvement with natural cellular procedures. Heterocyclic compounds do have a substantial role in arranging biological efficacies. This is moreover appeared when 2'-amino-4-chlorobenzophenone and 4-aminoantipyrine based Schiff base metal complexes shows good antibacterial efficacy as they include heterocyclic moiety. Relatively, this efficacy is highly consolidated for the metal complexes created from 2'-amino-4-chlorobenzophenone and 4-aminoantipyrine. The antimicrobial efficacy of the complexes obeys the order Cd < Zn< Ni < Cu< Co <Mn that may be result to the growing constancy of the complexes.

In vitro cytotoxicity

The cytotoxicity (in vitro) was estimated incubation of the preparation components after 24 hrs at growing concentration with the cancer and normal cells. Outcomes of the MTT screening are elucidated in phrase1s of concentration desired for(IC 50%) 50% inhibition existed in Graph 1. The components displayed cytotoxic efficiency versus each of two cell lines at a concentration was so low. In spite of $[Zn(TMAB)]Cl_2.H_2O$ and $[Ni(TMAB)]Cl_2.H_2O$ were more than leverage the cytotoxicity of $[Cd(TMAB)]Cl_2$, $Mn(TMAB)(H_2O)_2]Cl_2.H_2O$ and $[Co(TMAB)(H_2O)_2]$ $Cl_2.2H_2O$. Cytotoxic effective of $[Cu(TMAB)(H_2O)_2]Cl_2$ was partially greater for hep 2 cancerous cells while liken with the infected cell. The cytotoxic influence measured inspected utilizing the acridine orange smearing. Evident morphological shifts were spotted in the processed cells as a drop- entrusted manner liken to the solvent processed cells. Both cell lines uncovered to the components displayed compressed chromatin and occurrence of apoptotic bodies as apoptotic signals [25]. Moreover, the digit of binucleated and micronucleated cells were dramatically raised after the processing with compounds .Moreover, the influence of $[Cu(TMAB)(H_2O)_2]Cl_2$ was got to be powerful than the other components until its minimize concentrations. This was harmonious with the products of the MTT screening.

DNA Cleavage

DNA cleavage studies show that Cu(II), Co(II), Mn(II), Ni(II), Zn(II)and Cd(II) complex cleave the DNA molecule completely. Further, the results obtained against the DPPH radical confirmed that the complexes are more effective to arrest the formation of the DPPH radicals and the lower IC_{50} values observed in antioxidant assays did demonstrate that these complexes exhibited differential and selective effects to scavenge radicals and hence the potential as drugs to eliminate the radicals**.**

Table 1: Antibacterial activity data of ligand and complexes

Zone of Inhibition(mm)																				
Compound	[TMAB]			$Mn(TMAB)(H_2O)_2]Cl_2.H_2O$			$[Co(TMAB)(H_2O)_2]Cl_2.2H_2O$			$[Ni(TMAB)]Cl_2.2H_2O$			$[Cu(TMAB)(H_2O)_2]Cl_2$			$[Zn(TMAB)]Cl_2.H_2O$			DMSO	Antibiotic
Organisms	500	750	1000	500	750	1000	500	750	1000	500	750	1000	500	750	1000	500	750	1000		(1 mg/ml)
Candida albicans	6	7	8	7	8	10	8	8	10	8	10	11	12	13	14	13	14	15	-	8
Aspergillus flavus	7	6	8	9	9	11	6	9	9	7	9	9	10	11	12	11	12	11	-	9
Penicillium spp.	6	8	9	9	10	9	8	9	11	8	11	8	10	9	14	7	10	14	-	11
Aspergillus niger	6	5	8	7	6	7	7	7	8	8	8	8	9	11	12	9	11	11	-	6
Trichophyton	5	6	9	10	9	9	7	9	10	10	10	9	9	10	15	8	10	13	-	9

Table 2: Antifungal activity data of ligand and complexes

Zone of Inhibition(mm)																				
Compound	[TMAB]			$Mn(TMAB)(H_2O)_2]Cl_2.H_2O$			$[Co(TMAB)(H_2O)_2]Cl_2.2H_2O$			$[Ni(TMAB)]Cl_2.2H_2O$			$[Cu(TMAB)(H_2O)_2]Cl_2$			$[Zn(TMAB)]Cl_2.H_2O$			DMSO	Antibiotic
Organisms	500	750	1000	500	750	1000	500	750	1000	500	750	1000	500	750	1000	500	750	1000		(1 mg/ml)
E. coli	3	4	7	9	11	10	6	8	10	5	7	8	10	11	12	9	10	12	-	8
Vibrio spp.	7	8	8	11	13	14	8	9	8	7	8	9	9	9	14	8	12	13	-	10
Staphylococcus aureus	4	7	7	10	9	11	7	7	9	8	7	10	8	10	12	9	11	10	-	8
Pseudomonas aeroginosa	5	7	8	11	14	14	8	8	10	9	8	8	9	11	15	10	13	11	-	10
Bacillus spp.	6	5	6	12	13	15	9	9	8	7	7	9	6	9	14	11	14	11	-	11
Vibrio parahaemolytics	3	4	8	9	12	13	8	7	9	8	8	8	8	8	14	13	12	10	-	8
Salmonella spp.	6	6	7	9	10	11	9	8	10	7	9	9	9	9	11	10	10	11	-	7
Aeromonas spp.	4	8	8	10	9	12	10	7	11	9	7	8	8	11	13	10	11	13	-	8
Klebsiella spp.	2	7	9	11	12	14	8	8	9	6	6	7	7	9	14	13	14	15	-	10
Proteus spp.	2	6	8	10	11	12	7	8	10	5	7	8	9	11	12	9	10	12	-	9

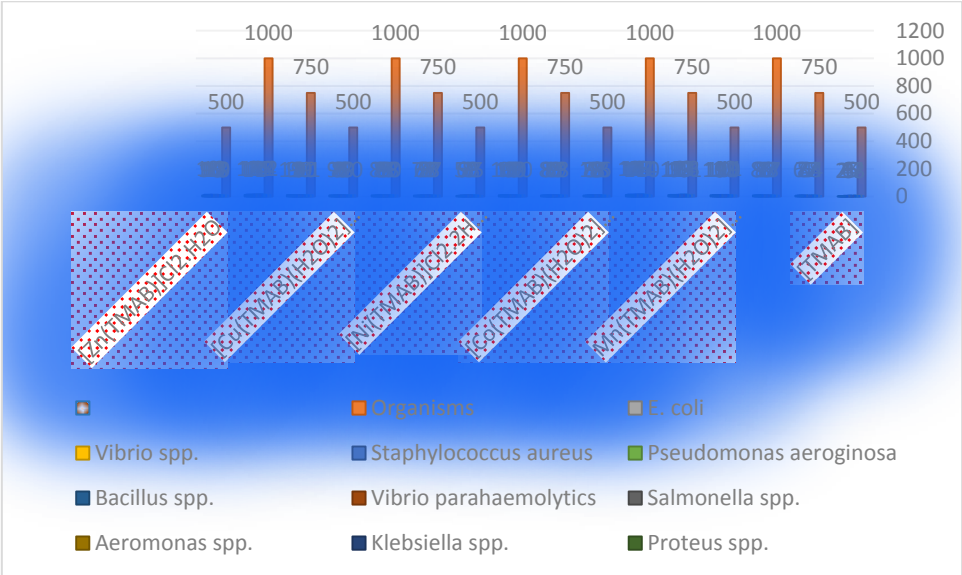

Fig. 1: Antibacterial activity of ligand and complexes

Table(3):The physical properties and microanalysis of all prepared products

Compound	Empirical Formula	(Formula wt.)	Yield %	Colour	Elemental Analyses Found (Calc.) %(calculated)				
					C	H	N	M	Cl
[TMAB]	$C_{27}H_{30}ClN_5O_5$	506.99	85	Off white	66.34 (64.35)	5.53 5.20)(	10.19 13.96)(	-	10.19 7.03)(
$Mn(TMAB)(H_2O)_2]Cl_2.H_2O$	$C_{27}H_{30}ClN_5O_5Mn$	738.53	67	Brown	64.88 (58. 55)	4.61 4.85)(	10.12 10.26)(	7.82 8.05)(	10.12 10.26)(
$[Co(TMAB)(H_2O)_2]Cl_2.2H_2O$	$C_{27}H_{30}ClN_5O_5Co$	686.18	65	Olive	64.26 (64.72)	4.21 (4.84)	10.07 (10.20)	8.34 (8.58)	10.07 (10.20)
$[Ni(TMAB)]Cl_2.2H_2O$	$C_{27}H_{26}Cl_3Ni\ N_5O_3$	6996.18	71	Pale green	64.43 (64.75)	4.23 4.85)(	9.87 10.20)(	8.17 8.55)(	9.87 10.20)(
$[Cu(TMAB)(H_2O)_2]Cl_2$	$C_{27}H_{30}ClN_5O_5Cu$	691.25	69	Green	63.71` (64.29)	4.45 4.81)(	10.02 10.13)(	9.05 9.19)(	10.02 10.13)(
$[Zn(TMAB)]Cl_2.H_2O$	$C_{27}H_{30}ClN_5O_5Zn$	691.18	80	Yellow	63.82 (64.12)	4.22 (4.80)	8.11 (10.10)	8.49 (9.43)	8.11 (10.10)
$[Cd(TMAB)]Cl_2$	$C_{27}H_{30}ClN_5O_5Cd$	811.20	79	Yellow	59.86 (60.05)	4.44 4.49)(	9.15 (9.46)	15.03 15.19)(	9.15 (9.46)

Table (4). The FT-IR spectral data (cm^{-1}) of all the prepared compounds

Compound	υOH-(H_2O)	ν(N-H)$_{sym}$ ν(N-H)$_{asym}$	ν(C=N)$_{PYR.}$	ν(C=N) imine	ν(M-OH_2)	ν (M-N)	ν (M-O)
[TMAB]	-	3311 3271	1597 -	1638	-	-	-
$[Mn(TMAB)(H_2O)_2]Cl_2.H_2O$	3032-3328b	3351 3186	1561	1620	765	508 489	464 442
$[Co(TMAB)(H_2O)_2]Cl_2.2H_2O$	3077-3363b	3368 3262	1576	1623	754	543 519	470 440
$[Ni(TMAB)]Cl_2.H_2O$	-	3455 3352	1558	1627	761	512 496	457 434
$[Cu(TMAB)(H_2O)_2]Cl_2$	3053-339b	3468 3385	1562	1622	768	580 563	459 427
$[Zn(TMAB)]Cl_2.H_2O$	-	3460 3348	1558	1625	760	541 497	450 437
$[Cd(TMAB)]Cl_2$	-	3468 3353	1561	1624	759	524 498	468 446

Table (5) UV-Vis spectral and magnetic moments values (nm) of the compounds in DMSO

Compounds	λ nm	υ cm^{-1}	ε_{max} ($molar^{-1}.cm^{-1}$)	Transitions	μe_{ff} (BM)	geometry
[TMAB]	279 345	35842 28985	2111 2260	$\pi\rightarrow\pi^*$ $n\rightarrow\pi^*$	-	-
$[Mn(TMAB)(H_2O)_2]Cl_2.H_2O$	278 347 412 787	35971 28818 24271 12706	2021 2200 1432 21	L.F C.T $^6A_1g \rightarrow {}^4A_1g(G),Eg(G)$ $^6A_1g \rightarrow {}^4T_2g(G)$	5.67	Octahedral
$[Co(TMAB)(H_2O)_2]Cl_2.2H_2O$	277 334 401 687 762	36101 29940 24937 14556 13123	2400 1956 1508 7 6	L.F C.T $^4T_1g_{(F)}\rightarrow {}^4A_2g_{(P)}$ $^4T_1g_{(F)} \rightarrow {}^4A_2g_{(F)}$ $^4T_1g_{(F)} \rightarrow {}^4T_2g_{(F)}$	4.72	Octahedral
$[Ni(TMAB)]Cl_2.H_2O$	275 345 408 810	36363 28985 24509 12345	2315 1825 1339 20	L.F C.T $^3A_2g_{(F)}\rightarrow {}^3T_1g_{(P)}$ $^3A_2g_{(F)}\rightarrow {}^3T_1g_{(F)}$	Dia.	Square planar
$[Cu(TMAB)(H_2O)_2]Cl_2$	276 337 412 701 859	37453 29673 24271 14265 11641	2329 763 995 49 5	L.F C.T $^2B_1g \rightarrow {}^2A_1g$ $^2B_1g \rightarrow {}^2B_2g$ $^2B_1g \rightarrow {}^2A_1g$	1.83	Octahedral
$[Zn(TMAB)]Cl_2.H_2O$	273 340 419	36101 41666 23866	2463 1305 1687	L.F C.T C.T	Dia.	Square planar
$[Cd(TMAB)]Cl_2$	271 342 412	36900 29239 24271	2418 2238 1368	L.F C.T C.T	Dia.	Square planar

Table 6: Anticancer influence of $Cu(TMAB)(H_2O)_2]Cl_2$ on Hep2 cell line

Concentration (µg/ml)	Dilutions	Concentration (µg/ml)	Absorbance (O. D)	Cell viability (%)
1000	Neat	1000	0.07	11.23
500	1:1	500	0.15	25.12
250	1:2	250	0.22	32.45
125	1:4	125	0.27	43.27
.62.5	1:8	62.5	0.32	47.46
31.2	1:16	31.2	0.36	56.38
15.6	1:32	15.6	0.39	61.43
7.8	1:64	7.8	0.43	67.65
Cell control	Cell control	Cell control	0.65	102.34

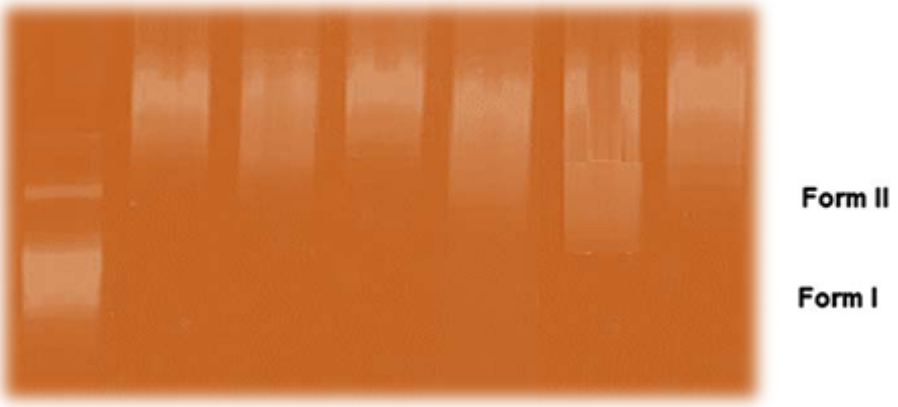

Figure 2

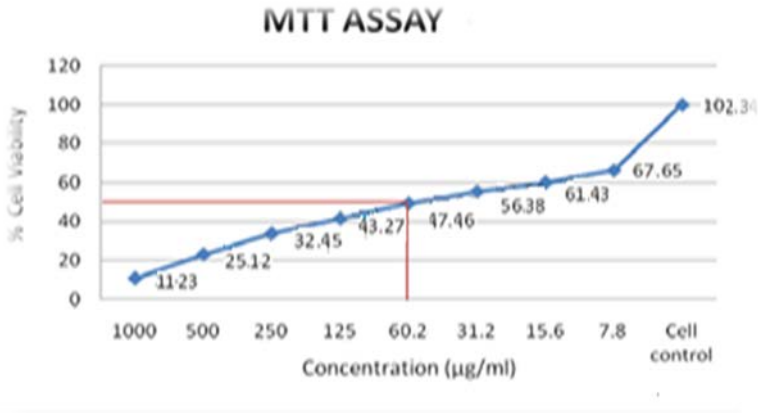

Figure 3: Anticancer influence of $Cu(TMAB)(H_2O)_2]Cl_2$ on Hep2 cell line

CONCLUSION

Possessed simultaneously, the preparation and spectroscopic description of a chains of $[Mn(TMAB)(H_2O)_2]Cl_2.H_2O$,$[Co(TMAB)(H_2O)_2]Cl_2.2H_2O$,$[Ni(TMAB)]Cl_2.2H_2O$, ,$[Cu(TMAB)(H_2O)_2]Cl_2$,$[Zn(TMAB)]Cl_2.H_2O$ and $[Cd(TMAB)]Cl_2$ complexes with a new Schiff base ligand obtained from 2'-amino-4-chlorobenzophenone and 4-aminoantipyrine. These complexes were described by utilizing various physico-chemical mechanisms. These complexes are all neuter, and set to square planar geometry for $[Ni(TMAB)]Cl_2.2H_2O$,$[Zn(TMAB)]Cl_2.H_2O$ and $[Cd(TMAB)]Cl_2$ octahedral geometry for $[Mn(TMAB)(H_2O)_2]Cl_2.H_2O$,$[Co(TMAB)(H_2O)_2]Cl_2.2H_2O$ and$[Cu(TMAB)(H_2O)_2]Cl_2$ complexes. The prepared compounds have antibacterial efficacy against (Staphylococcus aureus, Salmonella spp., E. coli, Vibrio spp., Pseudomonas aeroginosa, Vibrio parahaemolytics, Aeromonas spp., Klebsiella spp., Proteus spp., and Bacillus spp.) and also fungal efficacy against the (Aspergillus flavus, Aspergillus niger, Pencillium spp., Candida albicans, Trichophyton unlike the parent Schiff base ligand, the complexes displayed that considerable biological efficacy.

The complex $[Cu(TMAB)(H_2O)_2]Cl_2$ was more effective than the cytotoxicity of $[Mn(TMAB)(H_2O)_2]Cl_2.H_2O$,$[Co(TMAB)(H_2O)_2]Cl_2.2H_2O$,$[Ni(TMAB)]Cl_2.2H_2O$,$[Zn (TMAB)]Cl_2.H_2O$ and $[Cd(TMAB)]Cl_2$.Cytotoxic activity of $[Cu(TMAB)(H_2O)_2]Cl_2$ was somewhat higher for cancerous hep 2 cells when liken with the ordinary vero cell. The influence of $[Cu(TMAB)(H_2O)_2]Cl_2$ was set to be

stronger than the other compounds even at its lower concentrations. This was liken and deduced with the outcomes of the MTT assay. The compound $[Cu(TMAB)(H_2O)_2]Cl_2$ displayed the DNA fragmentation with a very agitated specific efficacy than the other complexes.

REFERENCES:

[1]. Tisato F, Refosco F, Bandoli G (1994) Structural survey of technetium complexes. Coord. Chem. 135: 325-397.

[2] Kumar, U. and Chandra, S.; J. Saudi Chem. Soc., 15, 187 (2011).

[3] Offiong, E.O., Emmanuel, N., Ayi, A.A. and Sante, M.; Transit. Metal Chem., 25, 369 (2000).

[4] Patil, R.M. and Chaurasiya, S.R.; Asian J. Chem., 20 (6), 4615 (2008).

[5] N. Demirezen, D. Tarınç, D. Polat, M. Çeşme, A. Gölcü, M. Tümer, Spectrochimica Acta A 94 (2012) 243– 255

[6] "Trimethoprim". The American Society of Health-System Pharmacists. Retrieved Aug 1, 2015..
cobalt(II), copper(II) and zinc(II) mixed-ligand complexes containing 1,10-phenanthroline and 2,2'-bipyridine. Bull. Chem. Soc. Ethiop., 24 (3), 383-389.

[9] Agwara M.O., Foba-Tendo J.N., Amah C., Yufanyi D.M., Ndosiri N.B., 2012. Thermogravimetric and antimicrobial properties of some divalent metal complexes of hexamethylenetramine. RJPBCS, 3(3), 95-104.

[10] Matangi S., Pragathi J., Bathini U., and Gyana K., 2012. Synthesis, characterization and antimicrobial activity of transition metal complexes of Schiff base ligand derived from 3-ethoxy salicylaldehyde and 2-(2-aminophenyl) 1-h-benzimidazole. E-J Chem., 9(4), 2516-2523.

[11] Alaghaz A.N.M.A., Farag R.S., Elnawawy M.A., Ekawy A.D.A., 2013. Synthesis and spectral characterization studies of new trimethoprim-diphenylphosphate metal complexes. Int. Jour. Sci. Res., 5 (1),

[28] Huheey, J.E. (1994) Inorganic Chemistry: Principles of Structure and Reactivity. Harper and Row Publisher, New York.

[29] Awetz, J., Melnick, P. and Delbrgs, A. (2007) Medical Microbiology. 4th Edition, McGraw Hill, New York.

[30] Priya, N.P., Arunachalam, S.V., Sathya, N., Chinnusamy, V. and Jayabalakrishnan, C. (2009) Catalytic and Antimicrobial Studies of Binuclear Ruthenium(III) Complexes, Containing Bis-β-Diketones. Transition Metal Che

Journal of Pharmaceutical Sciences & Research

JPSR

Journal of Pharmaceutical Sciences and Research

Scopus coverage years: from 2009 to Present

Publisher: PharmaInfo Publications

ISSN: 0975-1459

Subject area: Pharmacology, Toxicology and Pharmaceutics: Pharmaceutical Science

Visit Scopus Journal Metrics

CiteScore 2016 0.28

SJR 2016 0.158

SNIP 2016 0.391

http://www.scimagojr.com/journalsearch.php?q=19700174933&tip=sid&clean=0

http://www.jpsr.pharmainfo.in/Contact%20us.php

December 08, 2018

Dear Author(s)

Ref. No. JPSR DR9

Dr./Mr(s). Basima Abdul Hussin Zaidan/ University of Mustansiriyah, IRAQ
Dr./Mr(s). Noor M.Majee/ University of Baghdad, IRAQ
Dr./Mr(s). Rehab K. Al-Shemary/ University of Baghdad, IRAQ

Based on reviewer's recommendations, **I am delighted to inform you that your following manuscript** (JPSR DR9) **has been accepted for the publication in** (Journal of Pharmaceutical Sciences and Research (JPSR) ISSN: 0975–1459)

Title: Synthesis of some Schiff base metal complexes involving trimethoprim and 2'-amino-4-chlorobenzophenone: Spectral, thermal, DNA Cleavage antimicrobial,antifungal and Cytotoxic activity studies

Received In: October 09, 2018
Accepted on: December 08, 2018

Date of publication online: Vol:11 (No. 2) to get release in February 2019.
Plagiarism %: %

International Editorial Board
Dr. Ayad Alkaim
Please do not hesitate to contact me for further information
alkaimayad@gmail.com; Mobil and Viber: 00964-7801324986

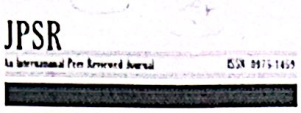

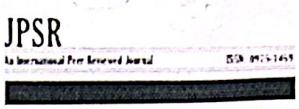

Journal of Pharmaceutical Sciences and Research

Scopus coverage years: from 2009 to Present

Publisher: PharmaInfo Publications

ISSN: 0975-1459

Subject area: Pharmacology, Toxicology and Pharmaceutics: Pharmaceutical Science

Visit Scopus Journal Metric

CiteScore 2016
0.28

SJR 2016
0.158

SNIP 2016
0.391

Kindly note Journal of Pharmaceutical Sciences and Research (JPSR) ISSN: 0975–1459*. It has* ***SCOPUS*** **h index 18** *(https://www.scimagojr.com/journalsearch.php?q=19700174933&tip=sid&clean=0)*

Thanks,

Regards,

International Editorial Board

Dr. Ayad Alkaim

Babylon University/ College of science for women

Please do not hesitate to contact me for further information

alkaimayad@gmail.com

Mobil and Viber: 00964-7801324986

Whats App: 00964-7801324986

Journal of Pharmaceutiical Sciences and Research

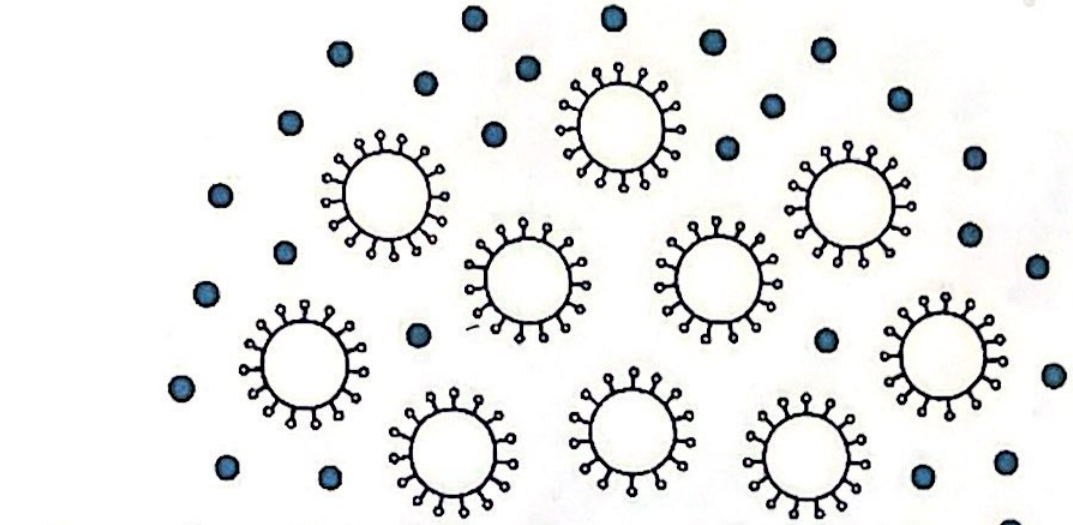

JPSR

An International Peer Reviewed Journal ISSN: 0975-1459